Advances in Technology Innovation, vol. 7, no. 2, 2022, pp. 92-104

Behavior of Built-Up Cold-Formed Steel Stub Columns Infilled with Washed Bottom Ash Concrete

Mohd Syahrul Hisyam Mohd Sani[1,*], Fadhluhartini Muftah[1], Nor Maslina Mohsan[1], Bishir Kado[2]

[1]School of Civil Engineering, College of Engineering, Universiti Teknologi MARA (UiTM) Cawangan Pahang, Bandar Jengka, Malaysia

[2]Department of Civil Engineering, Faculty of Engineering, Bayero University, Kano, Nigeria

Received 18 November 2021; received in revised form 25 January 2022; accepted 26 January 2022

DOI: https://doi.org/10.46604/aiti.2022.8933

Abstract

The main objective of the study is to determine the behavior of built-up cold-formed steel (CFS) stub columns infilled with washed bottom ash (WBA) concrete and also their failure mode. Five proportions of WBA as sand replacement in concrete and five specimens of built-up CFS stub columns infilled with WBA are produced in this study. There are four parts of the testing conducted: material properties of CFS, material properties of WBA concrete, mechanical properties of the connection, and mechanical behavior of built-up CFS stub columns. The result shows that the specimen with 25% WBA is reported to have the highest value of compressive strength in the material properties of WBA concrete and the mechanical behavior of built-up CFS stub column. The percentage difference of the ultimate load of the built-up CFS column filled with normal concrete and filled with WBA concrete is noted to have a range of 3% to 25%.

Keywords: built-up section, cold-formed steel, stub column, washed bottom ash concrete, buckling

1. Introduction

Cold-formed steel (CFS), sometimes identified as a thin-walled structure, is generally used as construction material either structural or non-structural element. CFS is produced by using steel sheets through a rolling process in ambient temperature, and is different from the hot-rolled steel produced by using high technology and huge machine in high temperature with an energy-consuming process. CFS is with many advantages such as being lightweight, ease of transportation, quick installation and erection, corrosion resistance, high strength to weight ratio, etc., and is normally utilized as a wall frame or panel, roof truss structure, and storage rack. CFS is formed in a variety of shapes, thicknesses, and cross-section areas, with the channel, hat, angle, and zee section normally found in the construction market. This section is becoming popular due to its ability for minimizing the total production or material cost. This popular section is classified as an open section which is common in the unsymmetrical section and exposed to structural integrity issues and failure.

The development of CFS is constantly changing in line with technological changes such as the production of complex shapes and cross-sections, enhancing the quality of steel material, producing corrosion resistance methods, and improvising methods of forming [1]. In overcoming the issue of structural integrity, this section is established by using a combination of two or more sections to produce the symmetrical section and sometimes it becomes a closed section. Selvaraj and Madhavan [2] mentioned about the CFS section with an unsymmetrical or single symmetrical or open section that failed due to the instability effect. Also, they mentioned that CFS is designed to transform to the built-up section which is classified as a close section or

* Corresponding author. E-mail address: msyahrul210@uitm.edu.my
Tel.: +60123267055

double symmetrical section. The new section which is recognized as the built-up section has existed in a variety of shapes, cross-section areas, and dimensions. The basic of the built-up section by using channel section is a back-to-back configuration or known as the I-section and face-to-face configuration or also as box-up or a hollow section. Fig. 1 illustrates the example of a built-up face-to-face and back-to-back CFS section by using a variety of sections.

Muftah et al. [3] reported the result of the behavior of built-up face-to-face CFS section with difference channel section which is fastened by using bolt and nut and known as outstand and extended stiffener under bending load. By producing the built-up section, the production cost of the section can be reduced and the cost of using an expert and high technology machine can be reduced. The build-up section is formed by using a variety of fasteners or connectors, for instance, bolt and nut, full welding, spot welding, self-tapping screw, self-drilling screw, rivet, and innovation fastener. Li et al. [4] have stated that the compression capacity in the axial condition of the built-up column section is allowed twice and more than twice of the basic section in producing the closed or symmetrical section. Nie et al. [5] mentioned that there are a lot of researchers who studied screw spacing and thickness effect on the strength of built-up back-to-back CFS columns that are broadly utilized in engineering activity due to quick assembly and installation. Meza et al. [6] stated that the performance and fundamental knowledge of built-up CFS columns are still limited.

The main objective of the study is to determine the mechanical behavior of the built-up CFS columns under compression load and observe the failure mode of the columns. Furthermore, the study is also to determine the suitable proportion which would provide the optimum mechanical behavior of built-up CFS columns with different proportions of the washed bottom ash (WBA) as sand replacement in concrete for solving the structural integrity issues and failures.

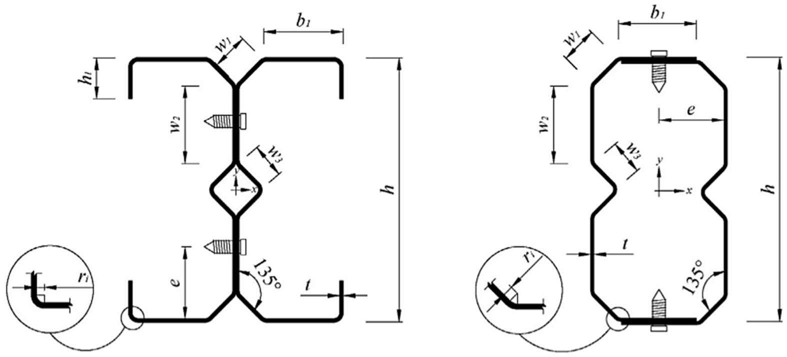

(a) Face-to-face and back-to-back [8]

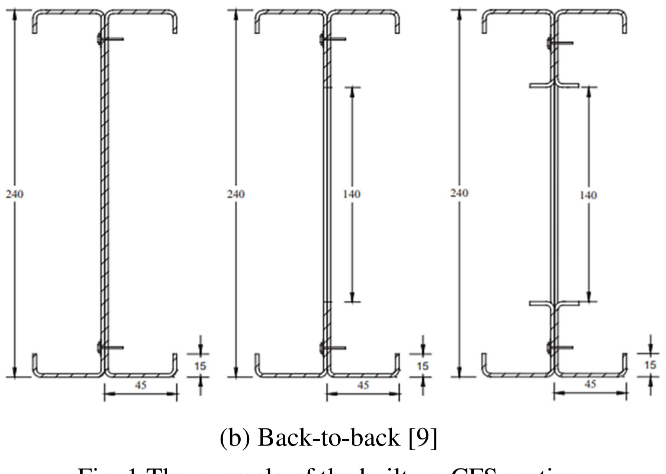

(b) Back-to-back [9]

Fig. 1 The example of the built-up CFS section

2. Built-Up Cold-Formed Steel Column

The built-up CFS column is normally provided of the mechanical behavior, especially the ultimate load value with twice or more than twice of the individual section under axial compression [4]. Roy and Lim [7] have reported the built-up face-to-face channel column which is classified as a hollow section with twice the strength of the individual section, and have promoted that the stability of the section is suitable to use in frames. In American Iron and Steel Institute (AISI S100-16) and Australia and New Zealand (AS/NZ) Specification, the built-up CFS section is designed by modifying the slenderness ratio $(KL/r)_m$:

$$\left(\frac{KL}{r}\right)_m = \sqrt{\left(\frac{KL}{r}\right)_o^2 + \left(\frac{a}{r_i}\right)^2} \tag{1}$$

where $(KL/r)_o$ is the overall slenderness ratio, a is the length of the intermediate fastener, and r_i is the radius of gyration (minimum).

CFS with a thin and slender section as compression or flexural member tends to have the buckling failure, such as local, distortional, global and lateral buckling, web crippling, and torsion when subjected to load. The local, distortional, global, and lateral buckling of the CFS section is illustrated in Fig. 2. Several factors involved in the buckling failure of the CFS section are the cross-section, shape, imperfection, slenderness ratio, and height. Normally, the column is divided by referring to the slenderness ratio into three categories: short, intermediate, and slender columns; the short column fails due to yielding, while the slender column fails due to buckling [10].

Rokilan and Mahendran [11] stated that the local buckling affected the CFS section to fail because the CFS section has a larger width-to-thickness ratio and is not similar to the hot-rolled steel section. Selvaraj and Madhavan [2] described that the individual CFS section, which is classified as an open or slender section, has failed in several ways such as local, distortional, and global buckling when the structural section is exposed to the instability conditions. Nie et al. [5] reported that local buckling and local-flexural buckling happened for the CFS closed section, and the built-up closed section with two channel sections could avoid the distortional buckling when subjected to compressive load. Li et al. [4] reported that the study on the mechanical behavior of the built-up CFS, especially the effect of the distortional buckling, is still limited, and no research has been discussed due to the complexity of the cross-section.

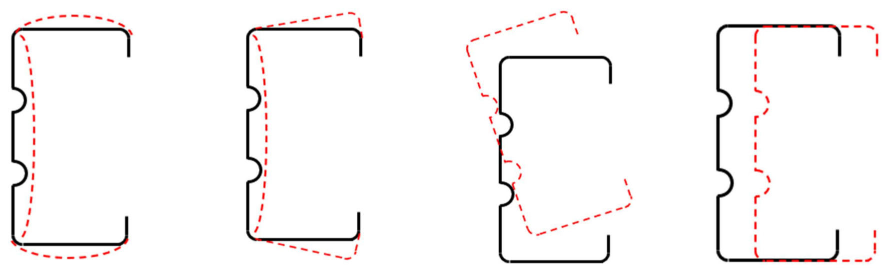
(a) Local (b) Distortional (c) Global (d) Lateral

Fig. 2 The buckling failure of the CFS section

3. Built-Up Cold-Formed Steel Column with Concrete

The built-up CFS incorporated with concrete and mortar as the column structure is increased due to an increase in the demand for the tall building construction. The composite structure is produced to be excellent in strength, buckling resistance, seismic resistance, and fire resistance, and is also capable to reduce the production cost and material cost. Ibanez et al. [12] reported that the combination of steel and concrete is broadly used in huge infrastructure and tall buildings because of its economic aspects, good structural behavior and bearing capacities, and better ductility.

The built-up CFS column with concrete can delay the deformation and crack of the concrete when subjected to axial compression, and acts as a permanent formwork that replaces the timber formwork. Zhu et al. [13] reported that the normal and self-consolidating concrete with a design strength of 30 MPa is utilized and filled into CFS tubes with 200 mm × 200 mm, square hollow section. Mohd Sani et al. [14] analyzed the resistance of the built-up face-to-face CFS column, which is fastened by bolt and nut and filled with normal concrete for the height of the column of 900 mm. Qu et al. [15] studied the axial compression behavior of the rectangular CFS tubes filled with concrete under two different loading methods. In design standard Eurocode 4, the plastic resistance to compression ($N_{pl,Rd}$) of the composite column based on the ultimate limit states is determined by the equation:

$$N_{pl,Rd} = \frac{A_a f_y}{\gamma_{Ma}} + A_c\left(\frac{0.85 f_{ck}}{\gamma_c}\right) + \frac{A_s f_{sk}}{\gamma_s} \quad (2)$$

where A_a is the cross-section areas of structural steel; A_c is the cross-section areas of concrete; A_s is the cross-section of reinforcement; f_y is the yield stress of steel; f_{ck} is the strength of concrete; f_{sk} is the yield stress of steel reinforcement; γ_{Ma}, γ_c, and γ_s are the partial safety factors at the ultimate limit states.

In general, the stub column or known as the short column is tested to obtain the structural behavior information as comprehensive and inclusive parametric studies to further assess the failure mode for considering varieties of the steel slenderness value and grades. Besides, when the length of the beam or slab is extended for any reason, the stub column is utilized as a structure and specifically acts as a concentrated point load which is designed and built above the beam. The stub column is sometimes planned as an interior aspect and utilized to improve the stability of the building. The testing of the stub column is conducted to evaluate the effect of the width-thickness ratio (b/t) on buckling behavior and bearing capacity.

Bottom ash (BA) is the waste product from coal-fired electric power plants which physically is lightweight and has a granular, porous, and coarsen surface. BA is collected from the furnace or boiler kiln at the bottom side, and another waste product, which is normally recognized as fly ash, is collected from the precipitator process. Normally, the total percentage of waste product of BA is more than the fly ash, and sometimes the BA is dumped at the nearest area for storing or recycling. If the BA is not properly stored, there will be environmental effects (such as air pollution, water pollution, and groundwater contamination) and human health effects (such as respiratory diseases and cancer risk) occurred imminently. Thus, BA is proposed for the 3R (Reduce, Reuse, and Recycle) process which is utilized as structural fill material, concrete ingredient material, and road base. BA with similar size of the sand is becoming popular to replace sand in concrete and lastly promoting the lightweight concrete. There is no information from previous studies on the utilization of BA filled in built-up CFS section as column or beam.

Nowadays, the normal concrete is shifted from traditional material to waste material which is parallel to the sustainable development program. The traditional material in normal concrete is replaced or substituted with waste material to solve the environmental problem which occurred from the beginning of the quarry activity. Mainly, the CO2 emission from aggregate occurred from the excavation, blasting, and transportation activities using electricity. Fayaz et al. [16] have noted that sand is scarce due to the Indian government imposing harsh restrictions on the sand quarrying at the river, which causes construction activities to be affected. The sand quarrying activities at the river normally produced environmental damage and river erosion [16]. Besides, sand mining activities have also created a lot of problems such as riverbeds becoming deeper, riverbank collapsed, vegetation losses on a riverbank and, aquatic life and agriculture sector interrupted [17]. They have also separated the aggregate into three categories, i.e., recycled coarse aggregate, normal coarse aggregate, and fine aggregate that are being used in concrete manufacturing which contributed to CO2 emission of 39%, 42%, and 19%, respectively.

From the observation and analysis, the information of the built-up CFS created with spot weld is still limited rather than other fasteners to form a symmetrical and closed section. Besides, the built-up CFS stub column infilled with normal concrete is considered a common of the study, but nowadays they are combined with special concrete for increasing the strength and improving the stability of the structure. The combination of built-up CFS with special concrete is recognized as new research activity and there is no code of practice that fully describes it. The arrangement and complete experimental setup for the built-up CFS stub column subjected to axial compression are not explained well in previous studies, especially the support condition and the imperfection analysis.

Previous studies have not enlightened the utilization of special concrete in the built-up CFS stub column as a structural component to reduce the overall weight and production cost of the structure, such as the optimum percentage of waste material for replacing the traditional material. Roy et al. [18] have reported that the information and design guidelines of the CFS stub column in the Australia-New Zealand code of practice (AS/NZS 4600) are classified as conservative when compared with a slender column. Roy et al. [19] stated that there are limited information and study on the determination of the strength due to axial compression for built-up face-to-face CFS and the effect of the spacing of the fastener. Ferhoune and Zeghiche [20] reported that very few studies by experiments have been conducted on the built-up CFS stub column which is with welding fastener and filled with normal concrete or special concrete.

4. Specimen Preparation and Experimental Setup

The CFS channel section with double intermediate web stiffeners and with a dimension of web element of 75 mm, flange elements of 34 mm, lipped element of 8 mm, the thickness of 1 mm, and steel grade of 550 MPa is selected as shown in Fig. 3. The section properties of the CFS channel section are tabulated in Table 1. CFS channel section is clean and clear before starting by checking the material properties of the section using a coupon tensile test specimen. CFS is cut on the web and flange elements which are situated vertically as similar as the column condition by referring to BS EN 10002-1:2001 [21]. Then, two CFS channel sections are located face to face to produce the built-up CFS section as same as the square hollow section by using spot weld on three locations as shown in Fig. 4. The spot weld with the width of 5 mm and with three numbers is located at the top, middle, and bottom of the built-up section in two parts (left and right) by referring to the study of Roy et al. [19]. The height of the specimens is constant at 250 mm.

The BA collected from the furnace or boiler kiln is prepared for the cleaning and washing process to form the WBA with appropriate sizes. For material properties of the WBA concrete, the concrete with grade 20 is designed by using material density and cast in 5 times accordingly to the proportion of sand replacement, 0%, 25%, 50%, 75%, and 100%. The total specimen of the concrete for material properties is 30 cubes, and the mix of all specimens is without using a superplasticizer. The concrete is cured in the water-curing tank for 7 days and 28 days of compressive strength. The built-up CFS section, as shown in Fig. 4(a), is filled with normal concrete as a control specimen and WBA concrete with 25%, 50%, 75%, and 100% to form a column. The total specimen of the built-up CFS column with WBA concrete is 12 specimens and 3 specimens with normal concrete. The built-up CFS with normal and WBA concrete is cured for 28 days before testing. The imperfection and residual stress of the CFS section are ignored in the study.

In the experimental activity, there are four parts which include material properties of CFS, material properties of WBA concrete, mechanical properties of the connection, and mechanical behavior of built-up CFS stub column. The universal testing machine (UTM) with a capacity of 30 kN is used for determining the material properties of the CFS test. The mechanical properties of connection are divided into two parts: shear connection and pull-out connection test. From the material properties of CFS, the ultimate strength, yield strength, elastic modulus, and deformation at ultimate load are observed. Furthermore, there are four specimens for the shear connection test and three specimens for the pull-out connection test proposed for checking the mechanical properties of the connection. The UTM with a capacity of 100 kN is utilized. The ultimate load of all connection test specimens is determined and the failure mode is observed.

Next, the material properties of the normal and WBA concrete, especially the ultimate load and compressive strength, are determined by using an auto compression machine with a capacity of 3000 kN. The failure mode of the concrete under compressive strength is observed. Lastly, for the mechanical behavior of the built-up CFS stub column, the ultimate load of the column is evaluated and the failure mode of the column for all proportions of WBA concrete is observed. The built-up CFS column without concrete is also determined for the comparison study. The experimental setup of the mechanical behavior of the built-up CFS stub column has followed the study of Mohd Sani and Muftah [22] as shown in Fig. 5.

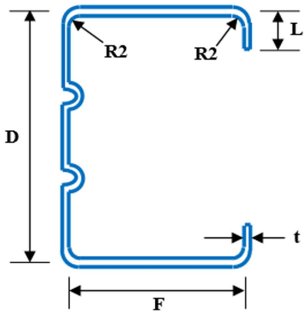

Fig. 3 The cross-section and dimension of the CFS channel section

Table 1 The section properties and dimensions of the CFS channel section

Parameter	Value and unit
Web (*D*)	75 mm
Lipped (*L*)	8 mm
Area (*A*)	148 mm^2
Second moment of area (I_{xx})	0.135 × 10^6 mm^4
Section modulus (Z_{xx})	3.605 × 10^3 mm^3
Radius of gyration (R_x)	30.22 mm
Flange (*F*)	34 mm
Thickness (*t*)	1 mm
Yield strength (f_y)	550 MPa
Second moment of area (I_{yy})	0.025 × 10^6 mm^4
Section modulus (Z_{yy})	2.240 × 10^3 mm^3
Radius of gyration (R_y)	12.94 mm

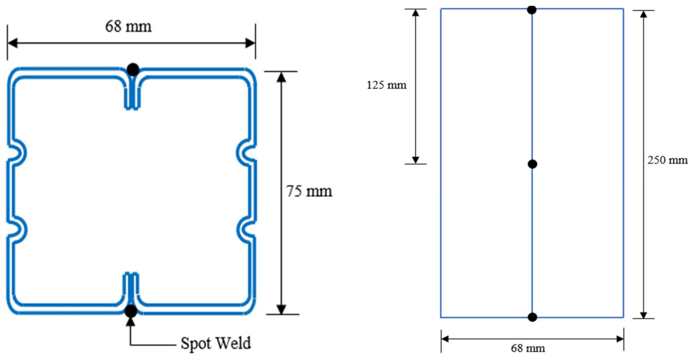

(a) Top (b) Front

Fig. 4 The view of the built-up CFS column

Fig. 5 Experimental setup for testing the mechanical behavior of the built-up CFS stub column

5. Results and Discussion

The results and discussion for the four parts of the experiment are analyzed here for achieving the objective of the study. The results and discussion are started with the material properties of CFS, continued with the material properties of WBA concrete and mechanical properties of the connection test, ending with the mechanical behavior of the built-up CFS stub column.

5.1. Material properties of cold-formed steel (CFS)

The result of the material properties of CFS is tabulated in Table 2. From the table, the highest value of the ultimate load is the flange element, and the lowest value of the ultimate load is recorded at the web element. The percentage difference of 5.89% for ultimate load, 5.88% for ultimate strength, 6.43% for yield stress, 2.44% for elastic modulus, and 4.06% for deformation at ultimate load are recorded between web and flange elements. The ultimate load and strength of the flange element are more than the web element because of the process of bending the flat element into a new element. The ultimate and yield strength is vividly increased from web to flange element due to strain hardening and cold-rolling process in the ambient temperature.

Besides, the increment is also due to cold-forming, which produces new strength, is added with existing strength, and decreases the ductility. Therefore, the ultimate load and strength of the element are dependent on the bending process. If the element is without a bending process, the ultimate load and strength would show the lowest value. The CFS which was bought from the Malaysia construction market has met the quality and is suitable for further work. Dinis et al. [23] reported that the elastic modulus of the web element is higher than the flange element when testing by using a coupon tensile specimen. Fig. 6 illustrates the example of the coupon specimen after failing, and Fig. 7 shows the stress-strain graph of the CFS.

Table 2 The result of the material properties of CFS

Element	Ultimate load (kN)	Ultimate strength (MPa)	Yield strength (MPa)	Elastic modulus (GPa)	Deformation at ultimate load (mm)
Web	6.71	536.6	524	205	4.43
Flange	7.13	570.1	560	200	4.25

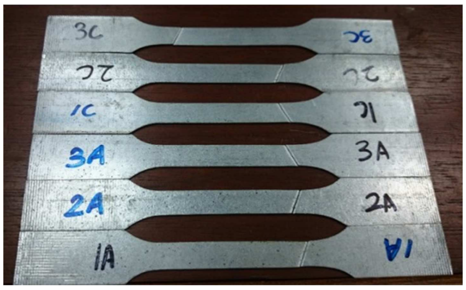

Fig. 6 The coupon specimen after testing

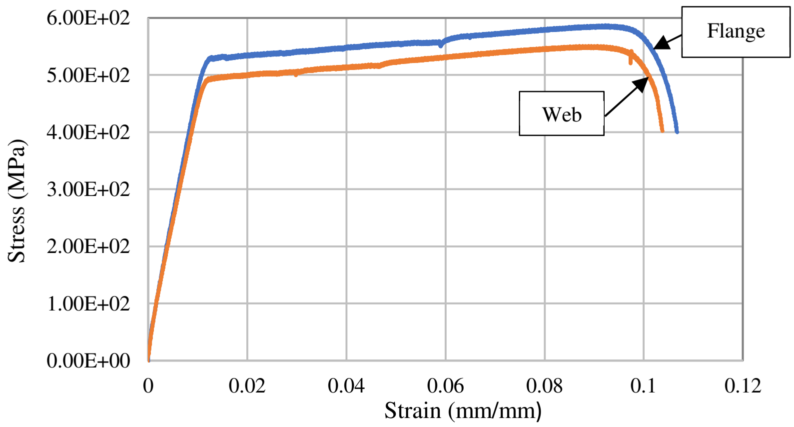

Fig. 7 The stress-strain graph of the material properties of CFS

5.2. *Material properties of washed bottom ash* (*WBA*) *concrete*

The material properties of WBA concrete, especially the ultimate load and compressive strength, are tabulated in Table 3. From the observation, the color of the specimen without WBA is brighter if compared with the specimen with WBA which shows dark grey. Fig. 8 and Fig. 9 illustrate the relationship between the compressive strength and the age of curing and the relationship between the compressive strength and the proportion of WBA, respectively. The highest and lowest value of compressive strength is 25% and 100% respectively of the WBA concrete specimen. The ultimate load and compressive strength of the WBA concrete are increased by increasing 25% WBA and decreased by increasing more than 25% WBA. This is because the WBA concrete with a high percentage of WBA has the fresh mix very dry and the hardened concrete too brittle.

The compressive strength of all specimens is increased from 7 days to 28 days as calculated approximately 24.26% of 0%, 26.15% of 25%, 25% of 50%, 21.05% of 75%, and 24% of 100%. The percentage achieved from the calculation is noted as significant and acceptable. The result of ultimate load and compressive strength with 25% WBA which is more than the control mix is similar to the study by Kim et al. [24]. Kim et al. [24] reported that the specimens with 25%, 50%, and 75% fine BA aggregate have shown more value of compressive strength compared with the control mix. The percentage difference of the compressive strength between all specimens with control is 7.34% of 25%, 18.81% of 50%, 71.78% of 75%, and 87.62% of 100% WBA concrete specimen. The failure mode of the 0% (control mix), 25%, 50%, and 75% are shown in Fig. 10. 100% WBA concrete specimen is classified as brittle concrete as shown in Fig. 11 with the overall side, and the corner of the cube is broken.

Table 3 The ultimate load and compressive strength of the WBA concrete specimen

Specimen	7 days		28 days	
	Ultimate load (kN)	Compressive strength (MPa)	Ultimate load (kN)	Compressive strength (MPa)
0% (control)	153.5	15.3	202.2	20.2
25%	160.7	16.1	218.7	21.8
50%	123.0	12.3	164.0	16.4
75%	44.9	4.5	57.56	5.7
100%	19.5	1.9	24.66	2.5

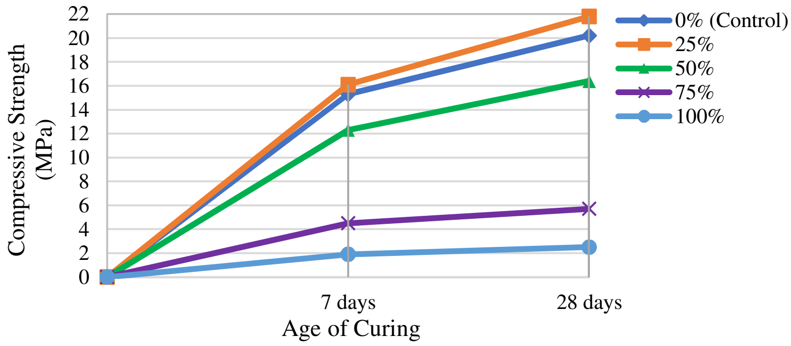

Fig. 8 The relationship of the compressive strength and the age of curing

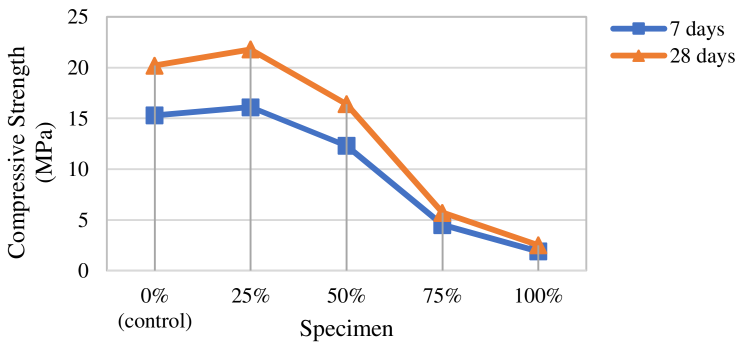

Fig. 9 The relationship of the compressive strength and different specimens

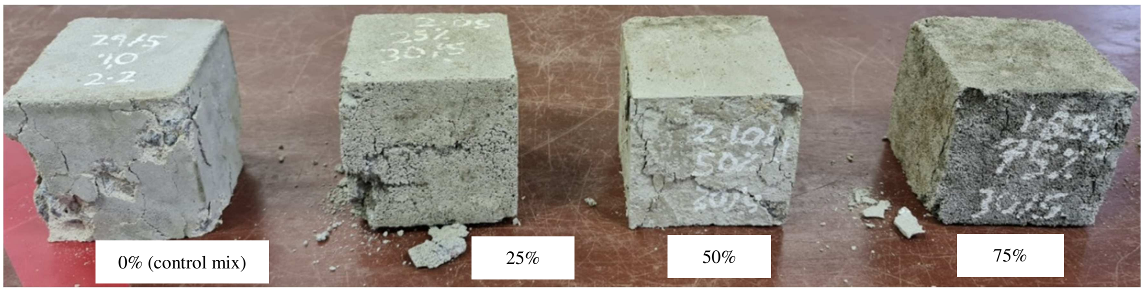

Fig. 10 The failure mode of specimen

Fig. 11 The failure mode of 100% WBA specimen after compressive strength test

5.3. Mechanical properties of the connection test

The shear connection test is conducted and the result is shown in Table 4. The percentage difference between the full weld and spot weld is determined and noted to have 77.49% for 1SW, 73.60% for 2SW, and 27.67% for 3SW. 68.87% and 63.50% are reported when the 3SW specimen is compared with 1SW and 2SW, respectively. 3SW is classified as an appropriate connection method for the built-up CFS section that gives the optimum value and shows the highest value of ultimate load with less energy consumption and less cost compared with the full weld method. The failure mode of all specimens is observed to have the break at the location of the weld. Fig. 12 illustrates the ultimate load between the methods of connection for shear testing. The graph illustrates that the ultimate load is increased by increasing the number of the spot weld.

The result of the pull-out connection test is tabulated in Table 5. Three specimens are tested and two-surface full weld (2SFW) specimens obtain the highest ultimate load value of 37.03 kN. The percentage differences between the three-number spot weld (3SW) specimen with 1SFW and 2SFW are 27.10% and 55.04%, respectively. The deformation at ultimate load between 3SW and 1SFW is illustrated similarly and the value is not too far between them, around 9.37%. The deformation at ultimate load for 2SFW is 10.64 mm and demonstrates that the connection with full weld at two surfaces is the most practical method to the joint between two sections. With the less deformation at ultimate load among the specimen, 2SFW is considered an appropriate connection method but the specimen is categorized as more costly and has high energy consumption when using full weld and compared with other connection methods. 3SW specimen is classified as a suitable connection method that provides a significant ultimate load for joining between two specimens without high cost and energy consumption. All specimens fail due to breaking at the weld.

Table 4 The shear connection test result

Specimen	Symbol	Ultimate load (kN)	Failure mode
Full weld	FW	13.37	Break at the weld
One-number of spot weld	1SW	3.01	Break at the weld
Two-number of spot weld	2SW	3.53	Break at the weld
Three-number of spot weld	3SW	9.67	Break at the weld

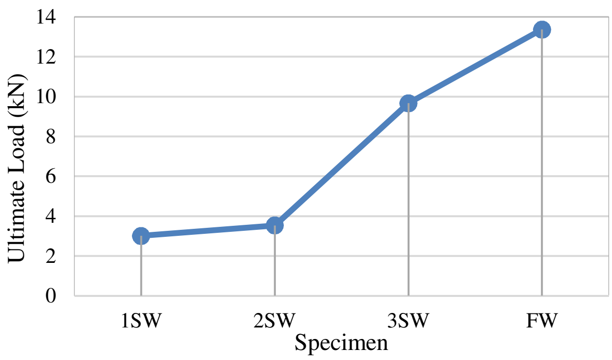

Fig. 12 The graph of the ultimate load according to the specimen or method of connection

Table 5 The pull-out connection test result

Specimen	Symbol	Ultimate load (kN)	Deformation at ultimate load (mm)
Three-number spot weld	3SW	16.65	25.14
One-surface full weld	1SFW	22.84	27.74
Two-surface full weld	2SFW	37.03	10.64

5.4. Mechanical behavior of built-up cold-formed steel (CFS) stub column

The mechanical behavior of the built-up CFS stub column is tabulated in Table 6 and Fig. 13. The highest value of the ultimate load and compressive strength is 25% WBA specimen, and the lowest value of the ultimate load and compressive strength is 100% WBA specimen. The ultimate load of the built-up CFS stub column without concrete is reported to have 73.5 kN. When the built-up CFS column is filled with normal concrete, the ultimate load is increased by around 55.86%. Although when the built-up CFS column is filled with WBA concrete with a different proportion, the ultimate load is improved approximately 66.53% of 25%, 54.148% of 50%, 48.24% of 75%, and 46.55% of 100% WBA specimen. The percentage difference of the ultimate load between the control specimens with WBA concrete is noted as having 24.18% for 25% WBA specimen, 3.72% for 50% WBA specimen, 14.72% for 75% WBA specimen, and 17.42% for 100% WBA specimen.

The failure mode of the specimen is also tabulated in the table and illustrated in Fig. 14. All specimens are observed to have local buckling and distortional buckling. Nie et al. [5] mentioned about the local buckling existing for the short column at web and flange elements when subjected to axial compression. The web and flange elements are deformed and moved out from the original as shown in the red circle in Fig. 15. The specimens do not fail at the connection area between one CFS channel with another CFS channel. The CFS section shows significant failure in buckling rather than concrete either normal or WBA concrete which does not illustrate the crack or failure as illustrated in Fig. 16. From the experimental activity, the built-up CFS with WBA concrete of 25% is shown as the specimen with optimum value, and the built-up CFS with WBA concrete of 50% is represented quite similar with control specimen. Besides, the 75% WBA and 100% WBA specimens are observed to fail on the surface of the column due to the brittleness of the WBA when fully replaced with sand. The pattern of the failure mode of all specimens is observed having the same condition and proven by previous studies, Nie et al. [5] and Nie et al. [25].

Table 6 The result of the mechanical behavior of the built-up CFS stub column

Specimen	Ultimate load (kN)	Compressive strength (MPa)	Failure mode
0% (control)	166.5	31.71	Local and distortional buckling
25%	219.6	41.83	Local and distortional buckling
50%	160.3	30.53	Local and distortional buckling
75%	142.0	27.05	Local and distortional buckling
100%	137.5	26.19	Local and distortional buckling

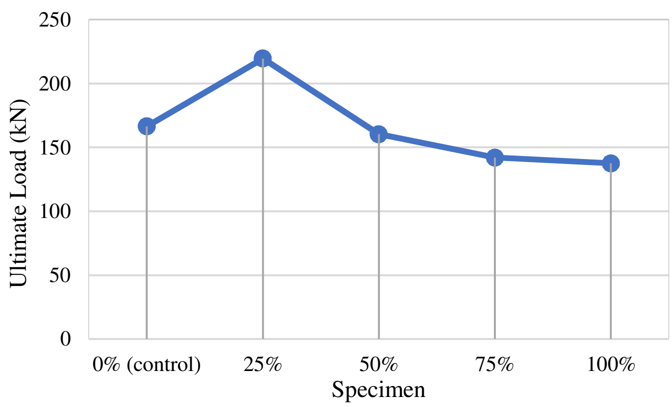

Fig. 13 The ultimate load of the built-up CFS column with different proportions of WBA concrete

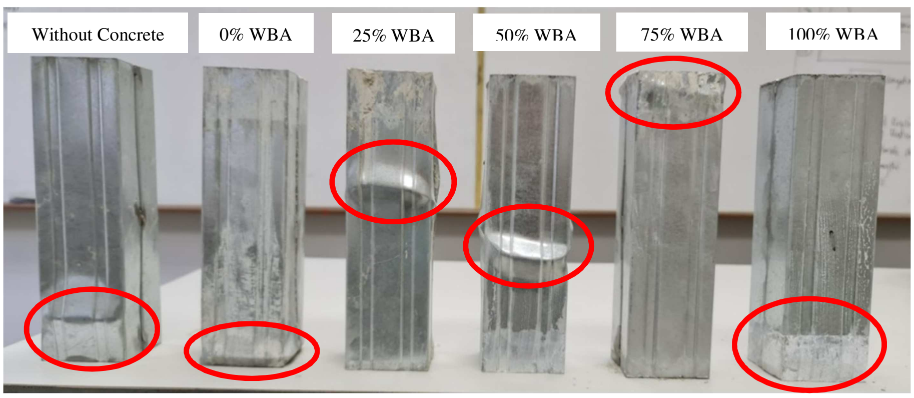

Fig. 14 The failure mode of the built-up CFS specimen from the front view

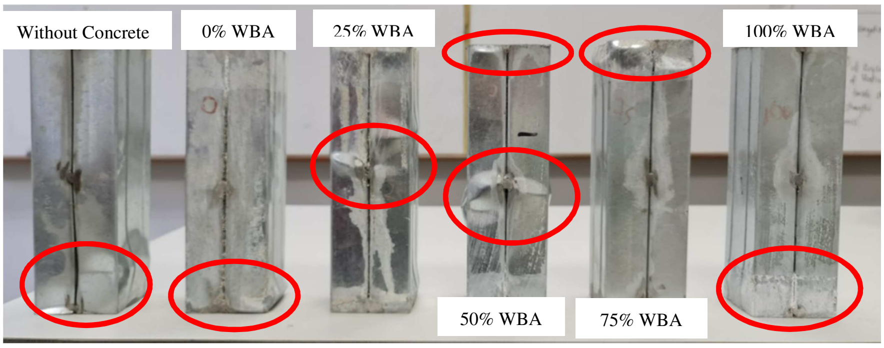

Fig. 15 The failure mode of the built-up CFS specimen at the connection area

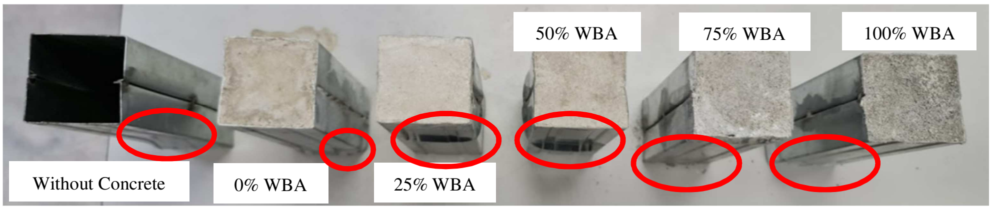

Fig. 16 The failure mode of the built-up CFS specimen from the top view

6. Conclusions and Recommendations

From the result and observation of the complete experimental activity, several conclusions and recommendations are drawn as shown here.

(1) The compressive strength of the WBA concrete with 25% of WBA is increased approximately 7.34% when compared with the control specimen. The result of compressive strength is increased between 21% and 26% when the concrete is fully submerged in water in early strength age with mature strength. The WBA concrete with more than 25% of WBA is shown to decrease and recorded to have 19% to 88% compared with the control mix. From the observation of the failure mode, the WBA concrete is noted to have brittle conditions when achieving more than 50% or until 100% of WBA.

(2) The built-up CFS stub column with 25% WBA concrete is shown to have the highest value of ultimate load and compressive strength with 219.6 kN and 41.83 MPa respectively and recorded to have 24.19% compared with the control specimen. The ultimate load and compressive strength of the built-up CFS column are increased when the WBA concrete is less than 25% and decreased when the WBA concrete is more than 25%.

(3) All specimens failed the local and distortional buckling on the steel surface, but there are no cracks or failure on the concrete surface detected. Thus, the utilization of 25% WBA as sand replacement can reduce the production cost and environmental problems produced from the site of the sand quarry.

For further study, the casting and mixing process of the fresh concrete must be added with the superplasticizer for controlling the strength and workability of the specimen. The built-up CFS intermediate and slender column should be designed and established to determine the relationship between the slenderness ratio and strength of the column. Lastly, the built-up CFS column with a variety of the fastener should be designed, produced, and discussed, and the imperfection aspect should be added in numerical analysis to evaluate the mechanical behavior.

Acknowledgements

The authors kindly thank the Malaysia Ministry of Higher Education under the Fundamental Research Grant Scheme (FRGS/1/2018/TK01/UITM/02/2) for the financial support and Universiti Teknologi MARA (UiTM) Cawangan Pahang for the facility support, especially laboratory machines and equipment. Sincerest gratitude is extended to the College of Engineering, UiTM Cawangan Pahang members and staff for providing technical assistance and advice.

Conflicts of Interest

The authors declare no conflict of interest.

References

[1] H. D. Craveiro, J. P. C. Rodrigues, and L. Laím, “Buckling Resistance of Axially Loaded Cold-Formed Steel Columns,” Thin-Walled Structures, vol. 106, pp. 358-375, September 2016.

[2] S. Selvaraj and M. Madhavan, “Design of Cold-Formed Steel Built-Up Columns Subjected to Local-Global Interactive Buckling Using Direct Strength Method,” Thin-Walled Structures, vol. 159, Article no. 107305, February 2021.

[3] F. Muftah, M. S. H. M. Sani, and M. M. M. Kamal, “Flexural Strength Behaviour of Bolted Built-Up Cold-Formed Steel Beam with Outstand and Extended Stiffener,” International Journal of Steel Structures, vol. 19, no. 3, pp. 719-732, September 2018.

[4] Y. Li, T. Zhou, L. Zhang, J. Ding, and X. Zhang, “Distortional Buckling Behaviour of Cold-Formed Steel Built-Up Closed Section Columns,” Thin-Walled Structures, vol. 166, Article no. 108069, September 2021.

[5] S. F. Nie, T. H. Zhou, Y. Zhang, and B. Liu, “Compressive Behavior of Built-Up Closed Box Section Columns Consisting of Two Cold-Formed Steel Channels,” Thin-Walled Structures, vol. 151, Article no. 106762, June 2020.

[6] F. J. Meza, J. Becque, and I. Hajirasouliha, “Experimental Study of Cold-Formed Steel Built-Up Columns,” Thin-Walled Structures, vol. 149, Article no. 106291, April 2020.

[7] K. Roy and J. B. P. Lim, “Numerical Investigation into the Buckling Behaviour of Face-to-Face Built-Up Cold-Formed Stainless Steel Channel Sections under Axial Compression,” Structures, vol. 20, pp. 42-73, August 2019.

[8] Q. Y. Li and B. Young, “Experimental and Numerical Investigation on Cold-Formed Steel Built-Up Section Pin-Ended Columns,” Thin-Walled Structures, vol. 170, Article no. 108444, January 2022.

[9] B. Chen, K. Roy, A. Uzzaman, G. Raftery, and J. B. P. Lim, “Axial Strength of Back-to-Back Cold-Formed Steel Channels with Edge-Stiffened Holes, Un-Stiffened Holes and Plain Webs,” Journal of Constructional Steel Research, vol. 174, Article no. 106313, August 2020.

[10] M. S. H. M. Sani, F. Muftah, and C. S. Tan, “Investigation on Mechanical Performance of Slender Cold-Formed Steel Channel Column,” Key Engineering Materials, vol. 706, pp. 107-111, August 2016.

[11] M. Rokilan and M. Mahendran, “Design of Cold-Formed Steel Columns Subject to Local Buckling at Elevated Temperatures,” Journal of Constructional Steel Research, vol. 179, Article no. 106539, April 2021.

[12] C. Ibanez, D. Hernández-Figueirido, and A. Piquer, “Effect of Steel Tube Thickness on the Behaviour of CFST Columns: Experimental Tests and Design Assessment,” Engineering Structures, vol. 230, Article no. 111687, January 2021.

[13] A. Zhu, X. Zhang, H. Zhu, J. Zhu, and Y. Lu, “Experimental Study of Concrete Filled Cold-Formed Steel Tubular Stub Columns,” Journal of Constructional Steel Research, vol. 134, pp. 17-27, July 2017.

[14] M. S. H. M. Sani, F. Muftah, M. F. Muda, and C. S. Tan, “Resistance of Built-Up Cold-Formed Steel Channel Columns Filled with Concrete,” Jurnal Teknologi, vol. 78, no. 5-2, pp. 99-104, May 2016.

[15] X. Qu, Z. H. Chen, and G. J. Sun, “Axial Behaviour of Rectangular Concrete-Filled Cold-Formed Steel Tubular Columns with Different Loading Methods,” Steel and Composite Structures, vol. 18, no. 1, pp. 71-90, January 2015.

[16] D. Fayaz, A. Malik, M. Zakir, and T. A. Malik, “Effects on the Properties of Concrete by Partial Replacement of Cement with Carbon Black and Natural Fine Aggregate with Robo Sand,” International Journal of Technical Innovation in Modern Engineering and Science, vol. 4, no. 6, pp. 1-8, June 2018.

[17] A. C. Sankh, P. M. Biradar, S. J. Naghathan, and M. B. Ishwargol, “Recent Trends in Replacement of Natural Sand with Different Alternatives,” Proceedings of the International Conference on Advances in Engineering and Technology, pp. 59-66, May 2014.

[18] K. Roy, T. C. H. Ting, H. H. Lau, R. Masood, R. Alyousef, H. Alabduljabbar, et al., “Cold-Formed Steel Lipped Channel Section Columns Undergoing Local-Overall Buckling Interaction,” International Journal of Steel Structures, vol. 21, no. 2, pp. 408-429, January 2021.

[19] K. Roy, C. Mohammadjani, and J. B. P. Lim, “Experimental and Numerical Investigation into the Behaviour of Face-to-Face Built-Up Cold-Formed Steel Channel Sections under Compression,” Thin-Walled Structures, vol. 134, pp. 291-309, October 2018

[20] N. Ferhoune and J. Zeghiche, “Experimental Behaviour of Concrete-Filled Rectangular Thin Welded Steel Stubs (Compression Load Case),” Comptes Rendus Mécanique, vol. 340, no. 3, pp. 156-164, 2012.

[21] Metallic Materials—Tensile Testing. Method of Test at Ambient Temperature, BS EN 10002-1:2001, 2001.

[22] M. S. H. M. Sani and F. Muftah, “Experimental Investigation of Built-Up Cold-Formed Steel Stub Column with and without Concrete-Filled,” AIP Conference Proceedings, vol. 2447, Article no. 020001, August 2021.

[23] P. B. Dinis, B. Young, and D. Camotim, “Local-Distortional Interaction in Cold-Formed Steel Rack-Section Columns,” Thin-Walled Structures, vol. 81, pp. 185-194, August 2014.

[24] Y. H. Kim, H. Y. Kim, K. H. Yang, and J. S. Ha, “Effect of Concrete Unit Weight on the Mechanical Properties of Bottom Ash Aggregate Concrete,” Construction and Building Materials, vol. 273, Article no. 121998, March 2021.

[25] S. Nie, T. Zhou, M. R. Eatherton, J. Li, and Y. Zhang, “Compressive Behaviour of Built-Up Double-Box Columns Consisting of Four Cold-Formed Steel Channels,” Engineering Structures, vol. 222, Article no. 111133, November 2020.

Copyright© by the authors. Licensee TAETI, Taiwan. This article is an open access article distributed under the terms and conditions of the Creative Commons Attribution (CC BY-NC) license (https://creativecommons.org/licenses/by-nc/4.0/).